

Seismic Displacement Capacity of Vulnerable Shallow Foundations

C. A. Blandon, J. F. Rave-Arango

Escuela de Ingeniería de Antioquia, Medellín-Colombia

A. R. Ortiz

Universidad de Medellín, Medellín-Colombia

J. P. Smith-Pardo

Seattle University, USA



SUMMARY:

Seismic evaluation and rehabilitation standards support the notion that the expected performance of a building under major ground motions largely depends on the deformation capacity of members and connections of the lateral-load-resisting system. But, while the importance of deformation demand/capacity in performance-based frameworks has been recognized for decades, there is still a major disconnect to this philosophy when it comes to soil-foundation systems because current seismic design/assessment standards only go as far as recognizing the finite stiffness and the finite bearing capacity of foundations with no consideration to their deformation capability. This paper describes the setup and preliminary results from an experimental program aimed at determining the seismic displacement capacity and energy dissipation characteristics of shallow foundation models on sand under combined axial load and moment. Preliminary results from the experimental program are used to define a beam-on-nonlinear-Winkler model that accounts for the limited deformation capacity of the bearing soil-foundation system. A case study of a building with vulnerable foundations -for which uplifting and reaching the bearing capacity of the supporting soil could occur during strong ground motions- is presented to discuss the implications of a limited deformation capacity for the foundations.

Keywords: soil-structure interaction; vulnerable foundation; performance-base framework; nonlinear analysis

1. INTRODUCTION

Documented studies on soil-structure interaction problems have existed for over a hundred years. Sir Lamb (1904), for instance, investigated the propagation of elastic waves induced by the application of a point load on the surface of an elastic semi-infinite media. But perhaps the most comprehensive presentation in decades of the theoretical and experimental research on vibration of foundations is a classic textbook by Richart et. al (1970).

In recent times, the dynamic response of footings has been described by using macro models and beam-on-nonlinear-Winkler models that capture the coupled nonlinear material and uplift response at the soil-foundation interface (Grange et al. 2009, Raychowdhury 2008). Experimental programs ranging from monotonic to cyclic loading and centrifuge tests have also been conducted to test some of these nonlinear formulations (Harden and Hutchinson 2009, Gajan et al. 2010).

Parallel to the development of soil-structure interaction models, seismic performance-based analysis and design of structures has become more widely accepted among structural engineering researchers and practitioners. The methodology relies on the definition of performance limit states that are, directly or indirectly, defined by experimental data. For example, the ultimate strain corresponding to crushing of unconfined concrete is conventionally (and in general, conservatively) taken as 0.003, but this value is supported by extensive experimental data and engineering judgment.

In contrast to performance-based methodologies, displacement/deformation limit states for soil-structure systems have not been established. While seismic rehabilitation standards (ASCE 41-06)

recognize the flexibility and limited bearing capacity of soil-foundations, no guidance is given in regards to the deformation capacity of foundations. Foundation deformation capacity can be critical to the seismic performance of structures because of the energy dissipation associated to yielding of the soil and period shifting associated to rocking and uplifting (Ugalde et al. 2010), however, drift demands may also be more significant.

This paper uses a numerical example to demonstrate that, for a particular type of soil used in the experimental program, foundation displacement demands for a seismically retrofitted building under strong ground motions are significantly less than the displacement capacity measured in the laboratory so the soil could serve as a mechanism to dissipate energy without compromising its load carrying capability.

2. BUILDINGS WITH VULNERABLE FOUNDATIONS

Foundation displacement capacity is relevant to the seismic performance of a building when foundations are prone to uplifting and/or to reaching the bearing capacity of the supporting soil during a strong ground motion. A practical case in which foundations can become vulnerable is illustrated in Fig. 1 and consists of a reinforced concrete moment frame building deemed to be inadequate for current code's seismic design provisions and subsequently rehabilitated through the installation of shear walls. In the original design, foundations are proportioned for demands that are consistent with the stiffness and strength of the columns and thus the bearing capacity of the soil is unlikely to be reached during a major seismic event (capacity protected foundation). But after placement of the shear walls and in absence of major modifications to the footings, the foundations under the walls may become vulnerable because they cannot fully transfer the large moment demands imposed by the stiff and strong slender members (Smith-Pardo 2008). Once it is determined that foundations are vulnerable, the critical issue is shifted to determining how much settlement and rotation the footings can sustain before losing their ability to carry load.

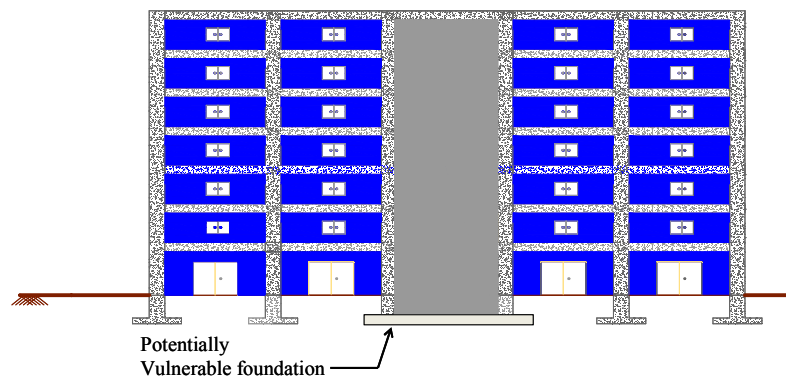


Figure 1. Building with vulnerable foundation

3. CODE-BASED APPROACH

Formulas and charts for the calculation of dynamic stiffness and damping of surface and embedded foundations of any shape may be found in seismic rehabilitation Standards ASCE 41-06. The foundation may be modeled by means of a set of elasto-plastic springs at the base of columns and walls. The static stiffness formulas are derived from elastic half space theory and in the case of rocking about the short axis of a footing, for example, the rotational stiffness is given by:

$$K_{\theta} = \frac{GB^3}{1-\nu} \left[0.4 \left(\frac{L}{B} \right) + 0.1 \right] \quad (3.1)$$

Where, B and L are the footing's width (perpendicular to the axis of rotation) and length; G and ν are the effective shear modulus and Poisson's ratio of the supporting soil.

ASCE 41-06 also recognizes the limited moment capacity of the foundation, which is calculated using Meyerhof's equivalent width concept; assuming that soil can fully plastify at the same level of stress under concentric and eccentric loading, the foundation moment capacity, M_n , for a constant axial load, P_n , can be proved to be given by:

$$M_n = P_n \frac{B}{2} \left(1 - \frac{P_n}{P_0} \right) \quad (3.2)$$

Where, P_0 is the bearing capacity under concentric loading and B is the foundation dimension in the direction of the applied moment

This moment-axial load interaction equation matches remarkably well the experimental results of footing models on sand under combined axial load and moment reported in several studies (Montrasio and Nova 1997, Georgiadis and Butterfield 1998, Smith-Pardo and Bobet 2007). The deficiency of the code formulation, once again, is that no consideration is given to the finite rotational capacity that the foundation may have.

4. NONLINEAR WINKLER MODEL AND TEST RESULTS

The average normal stress (σ_n) versus normalized settlement $\delta_n = \delta/B$ (where δ is the settlement from a concentric load test) response of a concentrically loaded shallow foundation may be used to define the springs for a nonlinear Winkler beam model of the same foundation but under combined axial load and moment. The use of normalized settlement is advantageous because it alleviates foundation size effects (Briaud and Gibbens 1999). Adjusting the response to a hyperbolic function, the relation can be written in terms of the initial slope, $K_{s0}B$, and the asymptote, σ_0 (which represents the bearing capacity stress under concentric loading) as follows:

$$\sigma_n = \frac{(K_{s0}B)\delta_n}{1 + \xi\delta_n} \quad (4.1)$$

where, ξ is the stiffness to strength ratio:

$$\xi = \frac{K_{s0}B}{\sigma_0} \quad (4.2)$$

Eq. (4.1) defines the force-settlement relation of nonlinear Winkler springs representing the stiffness of the supporting soil. The formulation is amenable to standard finite element programs such as SAP2000® which allows the user to define compression-only springs that obey any given force-displacement relation.

In order to show the capability of this nonlinear Winkler formulation, consider some of the large-scale soil-structure interaction experiments conducted in the project known as TRISEE (Negro et al. 2000). These involved the use of 1-meter square footings embedded to a depth of one meter in Ticino Sand ($D_{50}=0.55\text{mm}$; coefficient of uniformity, $C_u=1.6$; specific gravity, $G_s=2.68$; $e_{\min}=0.58$, $e_{\max}=0.93$). Two independent soil samples were used in the experimental program; one with a relative density of $D_R=0.45$ (low density, or "LD") and one with $D_R=0.85$ (high density, HD) were used.

Prior to the application of moment, small amplitude cycles under concentric load were applied in each case. The re-loading subgrade modulus for each soil sample was reported by Allotey and Naggar (2003) as $K_{s0}B = 280 \text{ MN/m}^2$ for the HD test and $K_{s0}B = 100 \text{ MN/m}^2$ for the LD test. A vertical load P

= 300 kN was subsequently applied to the HD test and P = 100 kN was applied to the LD test. The resulting safety factor under concentric loading alone was estimated to be 5.0 in both cases, therefore, $P_0 = 5P$ and so $\sigma_0 = 1.5\text{MPa}$ and 0.5MPa for the HD and LD soil respectively. Subsequent displacement-controlled cycles, with gradually increasing moment amplitudes and by keeping the axial load constant through the use of a system of air cushions, were applied until reaching the ultimate foundation resistance in each test.

Measured moment-rotation response envelopes (i.e., connecting the tips of the hysteretic loops) for the HD soil sample and for the LD soil samples are respectively shown in Fig. 2 and 3, together with the calculated response using SAP2000 by means of compression-only nonlinear springs whose axial behavior is defined by Eq. (4.1). It is observed that the comparison is favorable.

An estimate of the effective shear modulus was provided by Allotey and Nagaar as $G = 16\text{MPa}$ for HD soil sample and $G = 7.0\text{MPa}$ for LD soil sample. Assuming a Poisson ratio $\nu = 0.3$ in both cases, the rotational stiffness are calculated using Eq. 3.1 ($B/L=1$) as $K_0 = 11.4\text{MN-m}$ and 5.0MN-m for HD and LD soil sample respectively. Corresponding plastic moment capacities are calculated using Eq. 3.2 as $M_n = 120\text{kN-m}$ and 40kN-m . The resulting elasto-plastic relation based on elastic half-space theory is also indicated in Figs. 2 and 3.

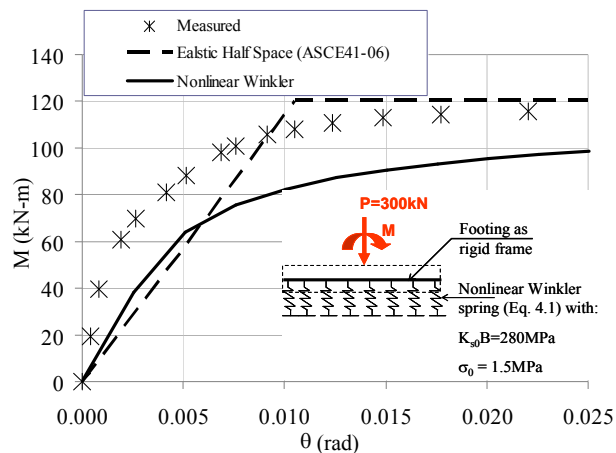


Figure 2. Moment-rotation response of large-scale foundation models, high density sand

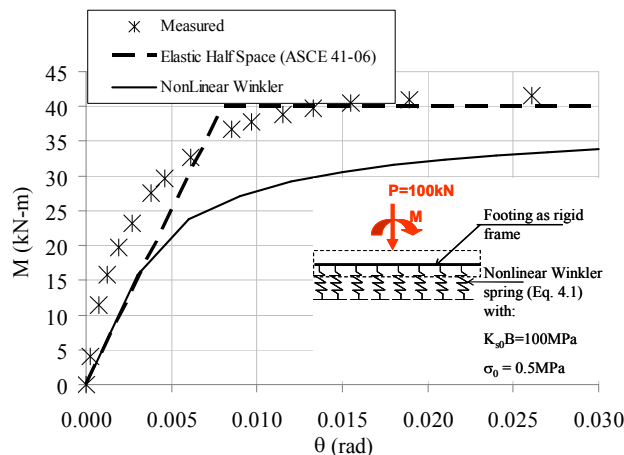


Figure 3. Moment-rotation response of large-scale foundation models, low density sand

5. EXPERIMENTAL PROGRAM

A 200-mm square by 25-mm thick steel plate has been used as the foundation model in the ongoing experimental program. The plate was placed on top of well-compacted fine sand and it was subjected to either axial load or a combination of axial load and moment. The experimental program has been divided into three test series as follows:

- Test Series I: The footing model is subject to concentric load only.
- Test Series II: The footing model is subject to varying moment, combined with a constant axial load, P . Cases considered include $P/P_0 = 0.2, 0.4, 0.5, 0.6,$ and 0.8 , where P_0 is the maximum concentric load measured in the concentric load tests (test series I).
- Test Series III: The footing model is subjected to combined axial load and moment by keeping the eccentricity, e , constant. Cases considered include $e/B = 1/10, 1/8, 1/6, 1/4,$ and $1/3$, where B is the footing model size (200-mm).

For each case, there are two actual tests being performed; a control monotonic and a cyclic test. This amounts to a total of 22 tests (two in Series I, ten in Series II and ten in Series III), all of them being displacement-controlled. In the monotonic tests, the displacement/rotation capacity is defined as that for which decay in the bearing capacity is observed. In the cyclic tests, two full cycles are applied at each level of a predetermined displacement history until loss of bearing capacity is observed (this would correspondingly define the displacement capacity of the footing model).

The general test setup and the loading apparatus are depicted in Fig. 4 for Test Series I and III (the setup for Test Series II is not described because of space limitations). The soil is placed in two wooden containers of 2.0x2.0-m and 1.0-meter deep. The use of two containers allows performing a companion cyclic test immediately after the corresponding monotonic test. The dimensions of each container were selected as to minimize boundary effects. The vertical load (concentric or eccentric) is applied to the footing model by means of a hydraulic actuator supported by a reaction beam. The reaction beam consists of two C10x20 steel sections supported by two 25-mm diameter threaded steel rods anchored to a strong floor. The magnitude of the vertical force is recorded using a 100kN-miniature compression load cell, while displacements and rotations are measured using linear potentiometers placed on the four corners of the plate. The level of resolution of the potentiometers is 0.0013mm.

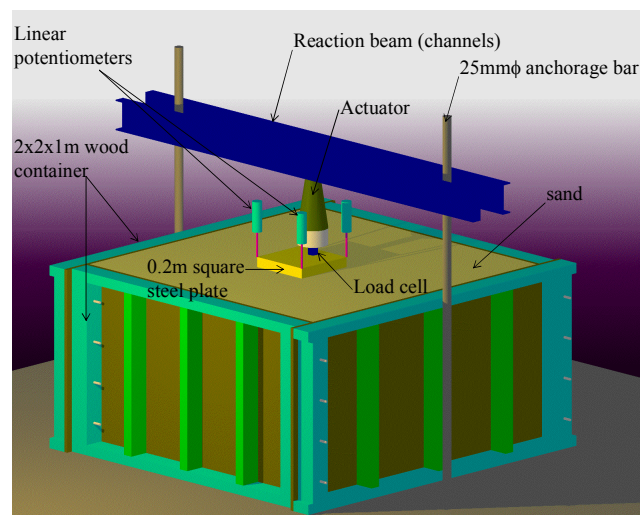


Figure 4. Setup for constant eccentricity and concentric tests

The test soil has a narrow particle size distribution obtained as determined with ASTM C 144-81. The corresponding USCS classification is a SP-SM poorly graded. The percentage of fines (passing sieve #200) was 11.4%. Minimum (ASTM D4254) and maximum density were measured to be 1.13 gr/cm³ and 1.52 gr/cm³. The test soil used was initially dried out, but because the experiments are being conducted outdoors the moisture content has fluctuated between 5 to 10%. For each test the container is fully emptied first and then the soil is placed and densified in layers of 10-cm by passing a 0.45x0.60m vibration plate compactor twice.

Fig. 5 shows the results for the foundation model under concentric axial load (monotonic) in terms of normalized variables together with a hyperbolic function fit given by Eq. (4.1) for which $K_{s0}B = 30\text{MPa}$ and $\sigma_0 = 1.0\text{MPa}$. Since the test was displacement-controlled, it is observed that the settlement capacity for this case is rather large (40% of the foundation model size). This is consistent with the observed punching shear failure but somewhat contradictory with the high densification of the sand that was achieved through compaction.

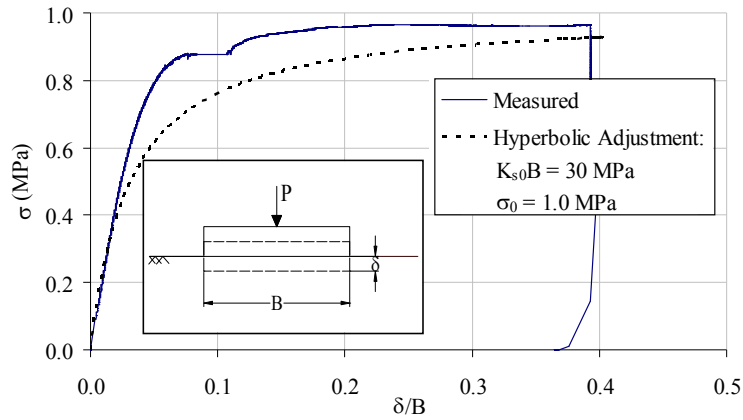


Figure 5. Test results for foundation model under concentric axial load

6. NUMERICAL EXAMPLE APPLICATION

Nonlinear time history responses were obtained for the numerical model of a reinforced concrete structure subjected to unidirectional seismic excitation. It was hypothetically assumed that the supporting soil for the building is identical to that in the undergoing experimental program of this research as characterized by Fig. 5 which included a bearing-capacity stress, σ_0 , equal to 1.0 MPa and an initial subgrade modulus $(K_{s0}B)_{\text{plate}} = 30\text{MPa}$. In order to account for size effects, the subgrade modulus for a footing of size B is calculated using an expression suggested by Terzaghi which relates the subgrade modulus from a 30-cm diameter standard plate, $K_{s\text{-plate}}$, with that of a full-size footing on cohesionless soil:

$$K_{s0}B = K_{s0\text{-plate}} \left(\frac{B + 0.30\text{m}}{2B} \right)^2 \quad (6.1)$$

where, B is the size (in meters) and K_{s0B} the subgrade modulus of the full size footing.

The foundation is modeled as nonlinear Winkler springs whose force-displacement relation is dictated by Eq. (4.1) with K_{s0B} given by Eq. (6.1). Takeda hysteresis rules are used to describe the behavior of the soil springs under load reversals.

The example structure corresponds to an actual four-story frame located in the city of Dinar-Turkey that was strengthened through reinforced concrete shear walls. The numerical model was subjected to twelve strong ground motion records whose response spectra are shown in Fig. 6. The records were

selected using the PEER ground motion database available online through the University of California at Berkeley.

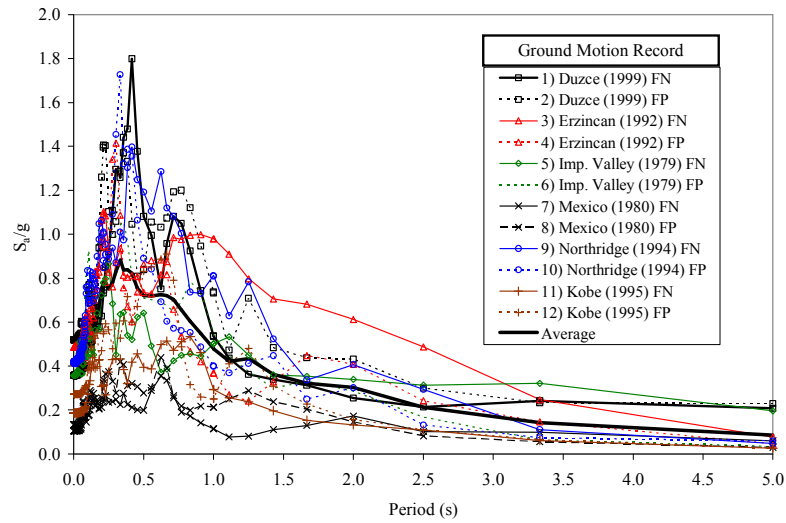


Figure 6. Ground motion records for nonlinear time history analysis of case structure

The general structural floor plan of the example structure is indicated in Fig. 7.a) and the corresponding structural model is shown in Fig. 7.b). The typical floor area is 310 m² (3340 ft²) and the story height is 3.8 m (12.5 ft) for the first floor and 3.5 m (11.5 ft) for the remaining floors. Cross sections are 0.25 x 0.60 m (10 x 24 in.) for columns and 0.25 x 0.70 m (10 x 28 in.) for beams, while reinforced concrete walls are 0.25 m-thick (10 in.). The compressive strength of concrete was only 12 MPa (1,700 psi) and the corresponding modulus of elasticity was calculated as 16,000 MPa (2,300 ksi) following section 8.5.1 of ACI 318-11. The specified yielding stress of the reinforcing steel was 220 MPa (32 ksi). The amount of longitudinal reinforcement in columns and walls was assumed equal to 1.0 and 0.2 percent of the respective cross-sectional area.

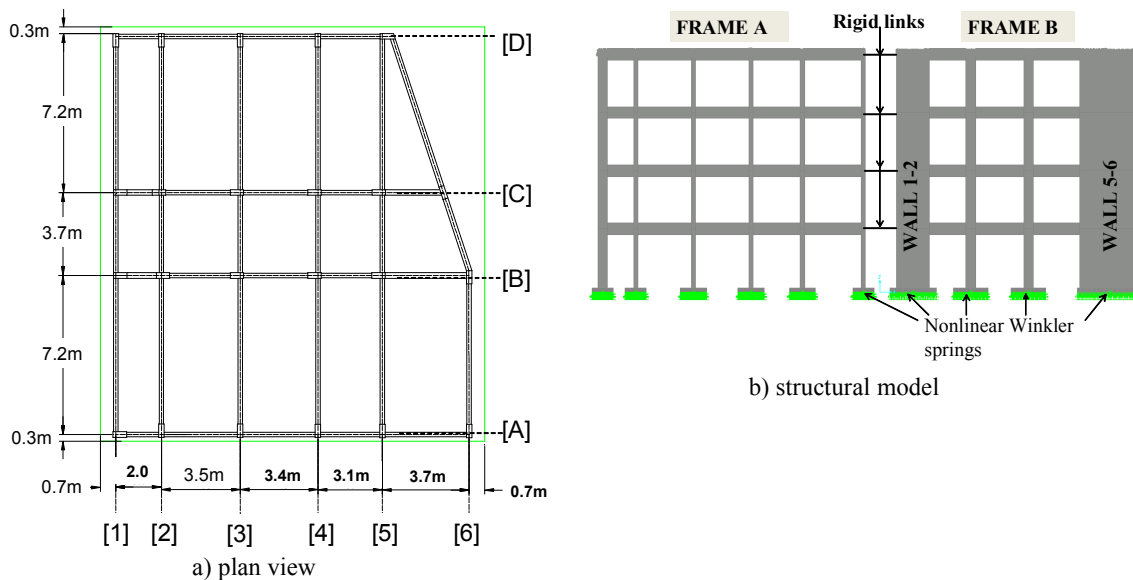


Figure 7. Plan view of and structural model of example building

A total story weight, including live load, equal to 1.0 ton/m² (200 lbs/ft²) and a minimum factor of safety of five against exceeding the bearing capacity of the soil ($\sigma_0 = 1.0$ MPa) were used to estimate the foundation sizes since actual dimensions were not known. The moment capacity of the foundations corresponding to axial forces due to gravity load was calculated using Eq. 3.2. Moment capacities for structural members, M_{ns} , were determined using conventional strain compatibility and a limiting concrete compressive strain equal to 0.003. Columns, beams and walls were assumed to exhibit an elastoplastic moment-curvature response with the linear portion given by the product of the modulus of elasticity of concrete and the cracked moment of inertia of the section. Only flexural hinges are assumed for the columns and variation of axial load with lateral excitation is neglected. For foundations, on the other hand, the interaction between axial load and moment is accounted for with the nonlinear Winkler springs

Table 1 summarizes the moment capacities used to define the nonlinear numerical model of the building. It is observed that the calculated moment capacities of reinforced concrete walls are significantly higher than those of the corresponding foundations. This implies that foundation uplifting and yielding of the supporting soil may occur before yielding at the base of walls; i.e., that foundations may be vulnerable.

Table 1. Model Parameters for Nonlinear Analysis of Four-Story Building

Frame	Axis	Column	Foundation	
		M_{ns} [kN-m]	B x L [mxm]	M_n [kN-m]
A	1	110	1.3 x 1.3	150
	2	50	1.3 x 1.3	180
	3, 4, 5	60	1.6 x 1.6	340
	6	45	1.3 x 1.3	170
B	3, 4	180	2.1 x 2.1	740
B (Walls)	1-2	1,800	2.8 x 1.2	760
	5-6	3,500	4.0 x 1.4	1,770
Beams	N/A	$M_n^+ = 150$ kN-m, $M_n^- = 150$ kN-m		

The numerical model of the building under the simulated ground motions was carried out using the computer program SAP2000®. It was assumed that the floor slabs provide full diaphragm action, and that proper reinforcement detailing precludes the occurrence of brittle modes of failures in shear or anchorage loss. In addition, because of the approximately symmetrical configuration of the structures, only frames A and B were considered in the two-dimensional analyses (Fig. 7). The structure was modeled as a wire frame with rigid offsets at the ends of the beams to account for the width of columns and walls.

The fundamental period of the structure was obtained to be equal to 1.0 second and the corresponding mass participation factor is 87%. From the nonlinear time history analysis, the maximum mean interstory drift ratio (lateral displacement at the roof divided by building height) is shown in Fig. 8.a) and corresponding nonlinear foundation rotation demand under the largest shear wall is shown in Fig. 8.b). It is of interest to notice that the maximum foundation rotation and the mean interstory drift ratio are very similar in magnitude thus indicating that minor distortion of the shear wall may be expected as a result of the vulnerable foundation.

Determination of foundation model rotational capacities for this particular soil is still an ongoing effort in the experimental program. However, previous research (Smith-Pardo, 2007) has indicated that 4-5% rotational capacity may easily be achieved on compacted sand, thus suggesting that the demands reported in Fig. 8 may not compromise the foundation moment capacity of the foundation.

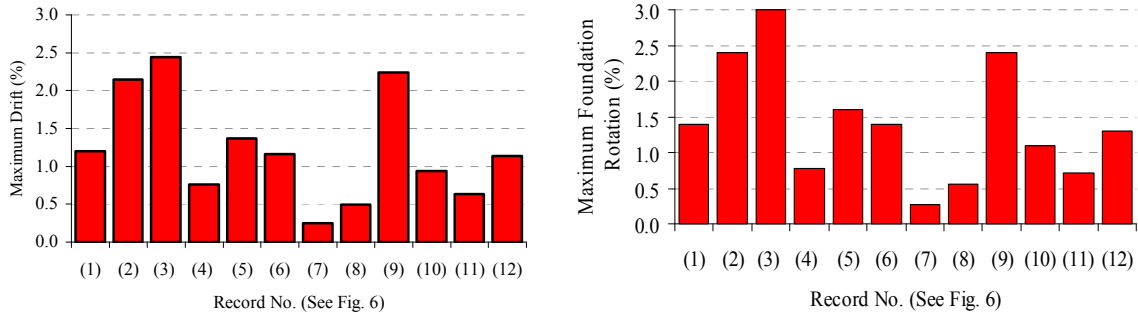
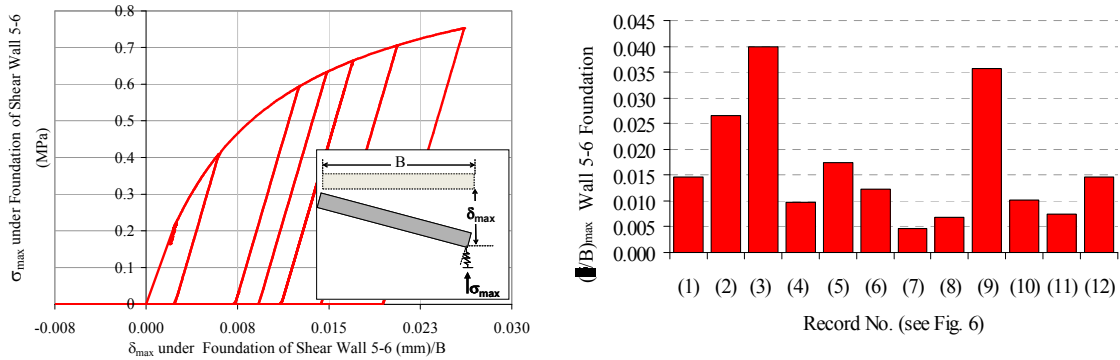


Figure 8. Maximum building drift ratio and wall 5-6 foundation rotation demand

Fig. 9.a) shows the maximum normalized settlement response at the edge of the foundation supporting the largest shear wall (Wall 5-6) when the building model is subject to record #2 (Duzce (1999) FP) shown in Fig. 6. In addition, a summary of the maximum foundation settlement normalized by the foundation size is also presented in Fig. 9.b).

Although a direct comparison with the displacement capacity observed in Fig. 5 is not quite correct, it is apparent that the maximum deformation demand δ/B obtained in the analysis (0.04) is nearly one order of magnitude smaller thus supporting the notion that shallow foundations may have ample deformation capacity and potential for energy dissipation through plastification of the supporting soil.



a) maximum foundation settlement under Duzce FP

b) maximum normalized foundation settlement under wall 5-6

Figure 9. Nonlinear Winkler spring behavior under shear wall 5-6

7. CONCLUSIONS

The use of nonlinear Winkler formulation characterized by the response of concentric loaded plates provides reasonable results for footings under combined axial load and moment. Preliminary results on a case study of a four-story building with vulnerable foundations suggest that a supporting soil with the same characteristics of that used in the experimental program of this study can have ample deformation capacity, well in excess of the deformation demand, and thus become a source of energy dissipation during a strong ground motion.

REFERENCES

- ACI 318-11 Building Code Requirements for Structural Concrete and Commentary, American Concrete Institute, Farmington, MI, USA.
- Allotey N, Nagaar M H. 2003. Analytical moment-rotation curves for rigid foundations based on a Winkler model, *Soil Dynamics and Earthquake Engrg.* **23(5)**:367-381
- ASCE SEI 41-06. 2006. Seismic Rehabilitation of Existing Buildings, American Society of Civil Engineers, Reston, VA
- Briaud J L, Gibbens R. 1999. Behavior of five large spread footings in sand. *J. Geotech. and Geoenviron. Eng.* **12(9)**:787-796.
- Gajan S, Raychowdhury P, Hutchinson T C, Kutter B L, Stewart J P. 2010. Application and validation of practical tools for nonlinear soil-foundation interaction analysis. *Earthquake Spectra, J. the Earthquake Engrg. Research Ins.* **26(1)**: 111-129
- Georgiadis, M. and Butterfield, R. 1999. Displacements of footings on sand under eccentric and inclined loads, *Canadian Geotechnical Journal*, **25(2)**: 199-211.
- Grange S, Kotronis P, Mazars J. A macro-element to simulate dynamic soil-structure interaction. *Engrg. Struct.*, 2009; **31(12)**: 3034-3046.
- Harden C W, Hutchinson T C. 2009. Beam-on-nonlinear-Winkler-foundation modeling of shallow, rocking-dominated footings. *Earthquake Spectra, J. the Earthquake Engrg. Research Ins.* **125(2)**: 277-300.
- Lamb H. 1904. On the propagation of tremors over the surface of elastic solid. *Philosophical transactions of the royal society of London*, **(203)**:1-42.
- Montrasio, L., and Nova, R. (1997), Settlement of shallow foundations on sand: geometrical effects, *Geotechnique*, **47(1)**, 46-60.
- Negro P, Paolucci R, Predetti S, Faccioli A E. 2000. Large-scale soil structure interaction experiments on sand under cyclic loading. *Proc. 12th World Conf. of Earthq. Eng.* Pub. No. 1191.
- Raychowdhury P. 2008. Nonlinear winkler-based shallow foundation model for performance assessment of seismically loaded structures. Ph.D. thesis. Univ. of California, San Diego, CA.
- Richart F E, Hall J R, and Woods R D. 1970. Vibrations of soils and foundations. Prentice-Hall Inc.
- Smith-Pardo J P, Bobet A. 2007. Behavior of rigid footings under combined axial load and moment. *ASCE J. Geotech. and Geoenviron.* **133(10)**: 1203-1215.
- Smith-Pardo, J. P. 2008. Reinforced concrete walls with vulnerable foundations. *ASCE J. Geotech. and Geoenviron. Engrg.*, **134(2)**:257-261.
- Ugalde, J. A, Kutter, B. L., and Jeremic B. 2010. Rocking Response of Bridges on Shallow Foundations. PEER Rep. No. 2010/101, Pacific Earthquake Engineering Research Center, Berkeley, CA